

IV. CONCLUSIONS

The behavior of the enhancement-factor and relaxation-times curves is well described by the drumhead model. Using the drumhead model for the domain wall the enhancement-factor magnitudes and behavior are derived from the equation of motion. The eddy-current damping appears to determine the magnitude of the domain-wall motion and thus the enhancement-factor behavior in pure Fe, whereas because of the increased resistivity and decreased saturation magnetization the stiffness

and damping effects appear to be comparable in the ordered alloys. The maximum enhancement factor is found to vary in the same manner as the initial permeability with alloying.

The nuclear relaxation appears to be via emission or absorption of a single bulk magnon, as was found to be the case in pure Fe. The relaxation times vary as much as a factor of 3 or 4 for different sites in the same alloy. This may reflect resonance or virtual magnon levels in the spin-wave spectrum.

- ¹M. B. Stearns, Phys. Rev. **129**, 1136 (1963).
²J. I. Budnick, S. Skalski, and T. J. Burch, J. Appl. Phys. **38**, 1137 (1967).
³M. B. Stearns, L. A. Feldkamp, and J. F. Ullrich, Phys. Letters **30A**, 443 (1969).
⁴M. B. Stearns, this issue, Phys. Rev. B **4**, 4069 (1971).
⁵M. B. Stearns, Phys. Rev. **162**, 496 (1967).
⁶M. B. Stearns, Phys. Rev. **187**, 648 (1969). Equation (4) is printed incorrectly; the exponential should be $e^{-2t(\text{sech}^2x)/T_{02}}$. However in evaluations of T_{02} the correct form was used.
⁷C. Kittel and J. G. Galt, in *Solid State Physics*, edited by F. Seitz and D. Turnbull (Academic, New York, 1956), Vol. 3, p. 437. Referred to as KG. See also M. Matsuura, H. Yasuoka, A. Hirai, and T. Hashi, J. Phys. Soc. Japan **17**, 1147 (1962).
⁸A. C. Gossard, A. M. Portis, M. Rubinstein, and R. H. Lundquist, Phys. Rev. **138**, A1415 (1965).
⁹K. H. Stewart, *Ferromagnetic Domains* (Cambridge U.P., Cambridge, England, 1954).
¹⁰F. W. Glaser and W. Ivanick, Trans. AIME **206**, 1290 (1956).
¹¹H. Matsumoto, 385th Report, Research Institute for Iron, Steel, and Other Metals, 1936 (unpublished).
¹²M. Fallot, Ann. Phys. **6**, 305 (1936).
¹³J. R. Asik and M. B. Stearns, Bull. Am. Phys. Soc. **16**, 403 (1971).
¹⁴T. Moriya, J. Phys. Soc. Japan **19**, 681 (1964); R. E. Walstedt, V. Jaccarino, and N. Kaplan, *ibid.* **21**, 1843 (1966).
¹⁵T. Wolfram and J. Callaway, Phys. Rev. **130**, 2207 (1963); T. Wolfram and W. Hall, *ibid.* **143**, 284 (1966); T. Wolfram, *ibid.* **182**, 573 (1969).

Luminescence of Neodymium in Barium Magnesium Germanate Crystals and Glass Hosts

Mohan Munasinghe* and Arthur Linz

Center for Materials Science and Engineering, and Department of Electrical Engineering, Massachusetts Institute of Technology, Cambridge, Massachusetts 02139

(Received 17 June 1971)

The optical properties of the rare-earth dopant neodymium in crystal and glass hosts of the identical chemical composition $\text{Ba}_2\text{MgGe}_2\text{O}_7$ have been studied on a comparative basis. This technique offers many advantages. Concentration quenching of emission is seen to commence at <1.0 at. % Nd^{3+} doping in the glass, but not at all for Nd^{3+} concentrations of up to ~2 at. % in the crystal. This and other related concentration- and temperature-dependent phenomena, including multiple-lifetime effects observed in the glass, are shown to be consistent with the existence of two predominant types of resonant-energy-transfer mechanisms between Nd^{3+} ions.

INTRODUCTION

In recent years stimulated emission has been reported in many solid-state hosts doped with various rare-earth ions.¹⁻³ In this group of activators, Nd^{3+} has been the most extensively used one. In this paper we present the results of an investigation of Nd^{3+} luminescence in crystal and glass hosts of identical chemical composition $\text{Ba}_2\text{MgGe}_2\text{O}_7$.

EXPERIMENTAL DETAILS

All the single crystals of $\text{Ba}_2\text{MgGe}_2\text{O}_7$ were grown by a top-seeded-solution technique.⁴ Glass samples were prepared by melting down a stoichiometric mixture of the required chemical composition and cooling it rapidly through the nucleation temperature.⁵ All samples were cut and polished to the same dimensions (approximately $5 \times 6 \times 7$ mm).

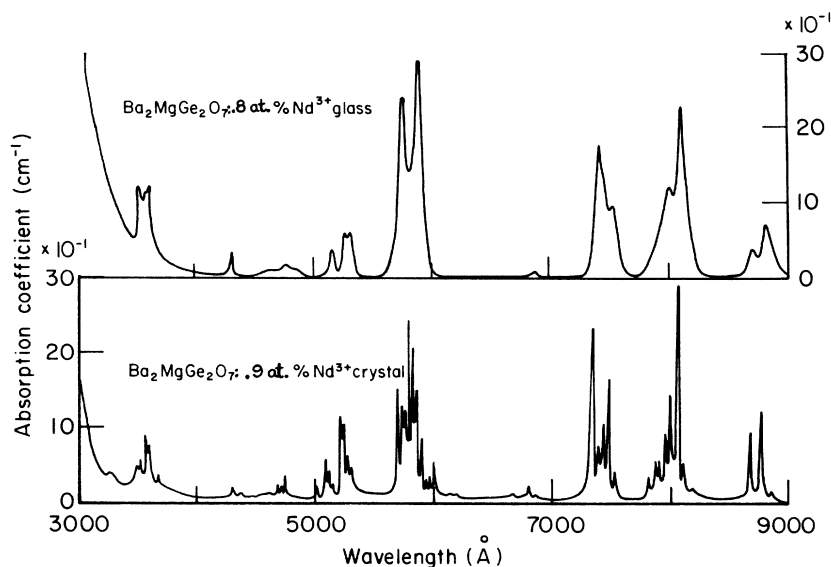


FIG. 1. Absorption spectrum of Nd^{3+} at 80°K.

Absorption measurements were made with Cary 14R and Beckman IR12 photometers. Fluorescence and excitation spectra were monitored with a Jarrell-Ash 0.5-m grating spectrometer and a S1 photomultiplier tube followed by a low-noise preamplifier, a lock-in amplifier, and a strip-chart recorder. A variety of optical pump sources, monochromators, and filters were also used when necessary. Lifetime measurements were made by exciting samples with a pulsed xenon source, feeding the preamplifier output directly into a fast-rise-time oscilloscope and photographing the trace. The pumping pulse had a duration of a few μsec which was much smaller than the smallest lifetime measured ($\sim 80 \mu\text{sec}$). A more comprehensive description of experimental details and results presented here is given elsewhere.⁵

RESULTS AND DISCUSSIONS

Figures 1 and 2 show typical absorption and emission spectra of Nd^{3+} -doped crystal and glass samples. All crystal spectra exhibited marked intensification and narrowing of both emission and absorption peaks as well as an increase in lifetime as the temperature was reduced from 300 to 80°K. Inhomogeneously broadened emission and absorption bands in glass were relatively unaffected by changes of temperature in the same range. Variations in activator concentration from 0.2 to 2% and from 0.2 to 10% atomic fraction⁶ in crystal and glass, respectively, had little effect on wavelength or linewidth in either host. Typical half-widths of lines at 80°K were $\sim 10 \text{ \AA}$ for crystal samples and $\sim 200 \text{ \AA}$ for glass samples.

The greatest Nd^{2+} absorption occurred at 0.805 μ and $\sim 0.58 \mu$ in crystal and glass, respectively,

while maximum emission occurred for the ${}^4F_{3/2} - {}^4I_{11/2}$ transitions at 1.054 and 1.065 μ . The Stark splitting of the fluorescent ${}^4F_{3/2}$ level in the crystal was 129 cm^{-1} .⁵

The barium magnesium germanate lattice belongs to the akermanite (i.e., $\text{Ca}_2\text{MgSi}_2\text{O}_7$) group. The ionic radii of the host matrix cations are $\text{Ba}^{2+} = 1.35 \text{ \AA}$, $\text{Mg}^{2+} = 0.65 \text{ \AA}$, and $\text{Ge}^{4+} = 0.53 \text{ \AA}$. Hence a Nd^{3+} ion of radius 1.08 \AA can be accommodated comfortably only in a Ba^{2+} site. The structural regularity of the doped crystal and purely exponential fluorescent lifetime indicate that the Nd^{3+} ions are incorporated substitutionally in Ba^{2+} cation sites. K^+ charge compensation is provided. The 4f electronic shell of the Nd^{3+} ion in which the fluorescent transitions occur is relatively well shielded from external perturbations. Thus shifts in corresponding energy levels of Nd^{3+} from one

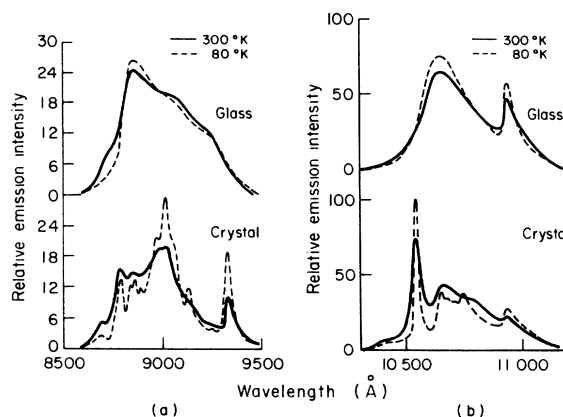


FIG. 2. Emission spectrum of Nd^{3+} at 80 and 300°K.

type of host to another are usually $\sim 100 \text{ cm}^{-1}$. However, in going from $\text{Ba}_2\text{MgGe}_2\text{O}_7$ crystal to glass, shifts in the centers of gravity of identifiable peaks were $\sim 25 \text{ cm}^{-1}$, indicating that the average change in site symmetry is not large.⁷ Temperature-insensitive inhomogeneous broadening due to a variety of slightly differing sites in $\text{Ba}_2\text{MgGe}_2\text{O}_7$ glass is typical of Nd^{3+} in other glasses^{1,2} as well. Some of the room-temperature broadening of crystal lines is caused by lattice phonons. A temperature-independent component of broadening which leads to linewidths $\sim 5 \text{ \AA}$ even at $\sim 5^\circ \text{ K}$ may be due to slight local disordering by the charge compensator.

The σ and δ (axial) spectra of Nd^{3+} in the crystal host were identical, indicating that electric dipole transitions were the dominant mechanism in both absorption and emission. The uv absorption edge for both hosts occurs at $\sim 0.34 \mu$, but excitation spectra showed that unlike certain other rare-earth-doped matrices⁸ there was no transfer of energy absorbed in this way, from the matrix to activators via ligand ions. Furthermore, for any given absorption line the absorption cross section was independent of Nd^{3+} concentration (i.e., Beer's law was obeyed⁹) in both hosts. Hence the oscillator strengths of Nd^{3+} transitions involving the $^4I_{9/2}$ ground state are independent of activator concentration in crystal and glass.

The quenching of Nd^{3+} fluorescence and lifetime as a function of activator concentration was studied. In the case of crystal samples no quenching of emission or lifetime of the excited state was evident for activator concentrations from 0.2 to 2% atomic fraction. Figures 3 and 4 clearly indicate effects of concentration quenching on the emission and lifetime, respectively, of the $^4F_{3/2}$ level of Nd^{3+} in glass. Quenching has already commenced at $< 1\%$ atomic fraction of Nd^{3+} concentration in both graphs.

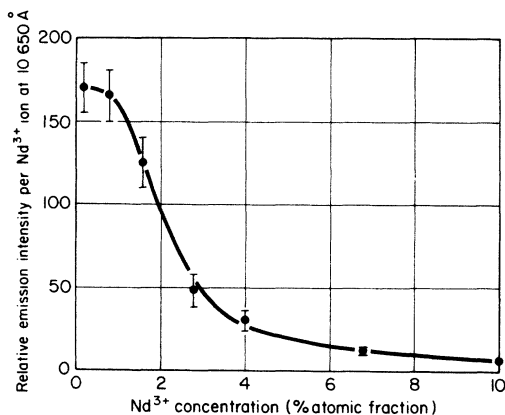


FIG. 3. Relative Nd^{3+} emission intensity per ion vs Nd^{3+} concentration in $\text{Ba}_2\text{MgGe}_2\text{O}_7$ glass at 300° K .

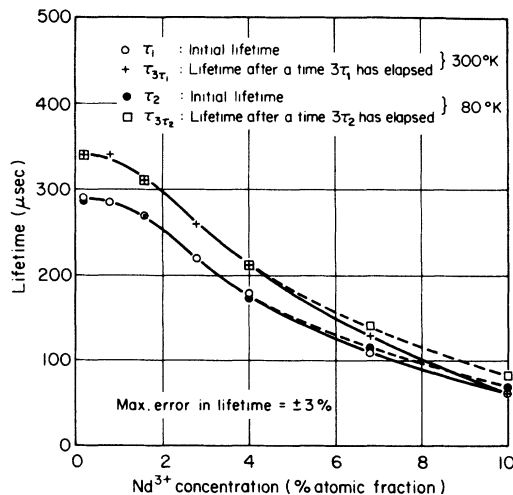


FIG. 4. Lifetime of $^4F_{3/2}$ level vs Nd^{3+} concentration in $\text{Ba}_2\text{MgGe}_2\text{O}_7$ glass.

There may exist in the glass a quenching mechanism of the type first postulated by Peterson and Bridenbaugh,^{10,11} involving the resonant transfer of energy. The process is illustrated in Fig. 5(a). Consider two Nd^{3+} ions A and B which are close to each other. Initially A is in the excited $^4F_{3/2}$ state while B is in the $^4I_{9/2}$ ground state. Ion A now transfers some of its energy to ion B so that finally both activators end up in the intermediate $^4I_{15/2}$ level; then rapid phonon decay¹² from this level down to a state lying between the $^4I_{15/2}$ and $^4I_{9/2}$ (e.g., the $^4I_{13/2}$ state) would complete the process, effectively killing the emission from the $^4F_{3/2}$ level of A. The transition probability for such a resonant transfer has been postulated to be of the form¹³⁻¹⁷

$$P_{AB}(R) \approx \frac{K}{R^\alpha} \int g_A(E) g_B(E) dE,$$

where R is the distance between activators, K is

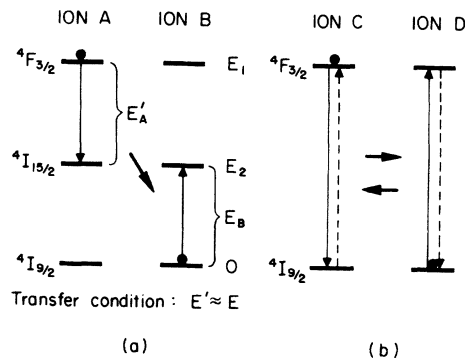


FIG. 5. Resonant energy transfer mechanisms between Nd^{3+} ions.

a constant depending on the type of resonant transfer (e.g., electric dipole, electric quadrupole, etc.), α is a constant ~ 6 to 10 depending on the type of resonant transfer, $g_A(E)$ is the normalized line shape of the ${}^4F_{3/2} \rightarrow {}^4I_{15/2}$ transition in ion A , and $g_B(E)$ is the normalized line shape of the ${}^4I_{9/2} \rightarrow {}^4I_{15/2}$ transition in ion B .

The functions $g_A(E)$ and $g_B(E)$ are approximately bell shaped and peaked at energies E_A and E_B , corresponding to the two respective transitions. Thus if $E_A \approx E_B$, the value of the overlap integral $J = \int g_A(E)g_B(E)dE$ would be significant, and provided that the ions were close enough (i.e., R small), the transfer probability P_{AB} could become much larger than the probability of photon emission P_E from the ${}^4F_{3/2}$ level of ion A . This would quench emission and fluorescent lifetime. On the other hand, if the energy mismatch $\Delta E = E_A - E_B$ were large, $J \rightarrow 0$. Hence $P_{AB} \ll P_E$ even for small interactivator distances R and normal photon emission would be the dominant deexcitation mechanism for excited activators such as A .

In $\text{Ba}_2\text{MgGe}_2\text{O}_7$ crystal, the energies of the top level of the ${}^4F_{3/2}$ manifold and the bottom level of the ${}^4I_{15/2}$ manifold with respect to the ${}^4I_{9/2}$ ground state are 11528 and 5838 cm^{-1} , respectively. Thus $E_A \approx 5690 \text{ cm}^{-1}$ and $E_B \approx 5840 \text{ cm}^{-1}$. Clearly even at 300°K the half-widths of $\sim 35 \text{ cm}^{-1}$ of the transitions involved would be insufficient to span the energy mismatch $\Delta E \approx 150 \text{ cm}^{-1}$ so that $J \rightarrow 0$, and $P_{AB} \rightarrow 0$ also. Thus in the crystal we would expect to find little evidence of quenching unless the activator concentration were very large, as confirmed by the experimental data. In any case, single crystals cannot be made to incorporate much more than $\sim 2\%$ atomic fraction of activator.

However, in $\text{Ba}_2\text{MgGe}_2\text{O}_7$ glass the energies of the centers of gravity of the ${}^4F_{3/2}$ and ${}^4I_{15/2}$ levels are 11500 and 5800 cm^{-1} , respectively. Thus $E_A \approx 5700 \text{ cm}^{-1}$ and $E_B \approx 5800 \text{ cm}^{-1}$, giving an energy mismatch of $\Delta E \approx 100 \text{ cm}^{-1}$. The half-widths of these transitions in glass $\sim 150 \text{ cm}^{-1}$ are large enough to span the energy mismatch so that $J \neq 0$ and hence $P_{AB} \neq 0$. In this case, as the activator concentration increases and the mean interactivator distance decreases, P_{AB} would become large causing significant concentration quenching effects. This is shown in the results. It should be noted that although the inhomogeneously broadened lines in glass are the envelope of many overlapping individual ionic lines, there would be a considerable number of neighboring activator pairs with a significant overlap integral J , especially at high concentrations.

Multiple-lifetime effects are a common feature of Nd^{3+} emission in all glasses^{2,3}. Owing to the variety of different activator sites in $\text{Ba}_2\text{MgGe}_2\text{O}_7$ glass we would expect to observe many lifetimes in any given

sample, as in Fig. 4. After the pumping pulse the decay of fluorescence from the aggregate of activators would be governed initially by the shortest lifetimes, while after some time had elapsed the longer lifetimes would predominate. In Fig. 4 the initial lifetime measured immediately after the pumping pulse, and the lifetime measured three initial lifetimes after the pumping pulse, yield an estimate of the spread of lifetimes in a given sample. By contrast, the corresponding decays in the crystal host were all pure exponentials.

In the following sections of the discussion we will present some evidence to show that the effects of activator concentration and temperature on multiple lifetimes Nd^{3+} in $\text{Ba}_2\text{MgGe}_2\text{O}_7$ glass are consistent with the presence of a resonant cross relaxation^{2,16} between neighboring Nd^{3+} ion pairs [see Fig. 5(b)]. The transfer probability for the reversible cross relaxation P_{CD} between activator ions C and D is governed by an equation similar to the one already given for the quenching resonant transfer probability P_{AB} . Since we are dealing with transitions between identical levels in both ions, the overlap integral J would in general be nonzero. At low-activator concentrations (i.e., large interionic distance R), P_{CD} would be small, the effect of the cross relaxation would be negligible, and multiple-lifetime effects could be clearly observed. However, as R decreased with increasing activator concentration, P_{CD} would also increase, strongly coupling together the ${}^4F_{3/2}$ levels of excited Nd^{3+} ions. The over-all decay rate would then tend toward that of the shortest-lived type of Nd^{3+} site.⁵ Therefore the spread of lifetime would decrease with increasing activator concentration.

Furthermore, as the temperature was decreased the overlap integral J between any given ion pair would in general decrease as a result of reduction in linewidth of the transitions. P_{CD} would also decrease, reducing the effectiveness of the cross relaxation. Thus at a given Nd^{3+} concentration the spread of lifetimes would be greater at lower temperatures. Also, the mean lifetime would be higher due to the reduced thermal decay rate. These effects are seen in Fig. 4. It should be noted that the cross relaxation would enhance quenching effects, as energy could hop from one activator to another until it finally reached a quenching site, such as a killer impurity or a coupled ion pair of the type discussed earlier.

CONCLUSIONS

This comparative study of Nd^{3+} fluorescence in $\text{Ba}_2\text{MgGe}_2\text{O}_7$ crystal and glass hosts has yielded important qualitative information on a number of possible mechanisms involved in the emission. The general technique of studying crystals and glasses

of identical chemical composition, doped with rare-earth activators, may be extended to many other hosts as well, provided, of course, that the glassy counterpart of the crystalline material can be successfully prepared in homogeneous pieces of sufficient size.

The use of rare-earth fluorescence as a probe under these circumstances simplifies the analysis of data considerably, particularly if it is done on a comparative basis, and offers the following advantages: First, various processes involved in luminescence such as energy transfer and quenching, occurring in these materials, can be better understood. Second, it is possible to investigate certain fundamental differences between the crystalline state characterized by its long-range order and the amorphous glassy state characterized by short-

range order only. The annealing of glass samples while emission is monitored at various stages in the recrystallization cycle is one possible technique. Our preliminary results suggest that further quantitative studies along these general lines should prove to be fruitful.

ACKNOWLEDGMENTS

The contributions of the following are gratefully acknowledged: V. Belruss, who grew all the crystals, J. Kalnajs, who helped in the gathering of spectroscopic data, Professor A. Smakula, H. P. Jenssen for useful discussions, and Mrs. Sria Munasinghe for typing and correcting the manuscript. This work was supported by the Office of Naval Research, Advanced Research Projects Agency, and Night Vision Laboratory, USAMERDC.

*Present address: Electrical Engineering Dept., McGill University, Montreal 110, P. Q., Canada.

¹G. O. Karapetyan and A. L. Reishakrit, *Izv. Akad. Nauk SSSR Neorgan. Materialy* **3**, 217 (1967).

²E. Snitzer, *Proc. IEEE* **54**, 1249 (1966).

³Z. J. Kiss and R. J. Pressley, *Proc. IEEE* **54**, 1236 (1966).

⁴A. Linz, V. Belruss, and C. S. Naiman, *J. Electrochem. Soc.* **112**, 60C (1965).

⁵Mohan Munasinghe, S. M. and E. E. thesis (MIT, 1969) unpublished).

⁶Atomic fraction = $N_a / (N_a + N_h) \approx N_a / N_h$, when $N_h \gg N_a$ and where N_a is the density of Nd^{3+} activator ions; N_h is the density of Ba^{2+} host matrix cation which is replaced by activator ions.

⁷C. Hirayama, *Phys. Chem. Glasses* **7**, 52 (1966).

⁸L. G. Van Uitert, *Luminescence of Inorganic Solids*

(Academic, New York, 1966), p. 484.

⁹D. W. Harper, *Phys. Chem. Glasses* **5**, 11 (1964).

¹⁰G. E. Peterson and P. M. Bridenbaugh, *J. Opt. Soc. Am.* **54**, 644 (1964).

¹¹Yu. K. Voronko and V. V. Osika, *Zh. Eksperim. i Teor. Fiz. Pis'ma v Redaktsiyu* **5**, 357 (1967) [*Sov. Phys. JETP Letters* **5**, 295 (1967)].

¹²M. J. Weber, *Physics of Quantum Electronics* (McGraw-Hill, New York, 1966), p. 350.

¹³D. L. Dexter, *J. Chem. Phys.* **21**, 836 (1953).

¹⁴D. L. Dexter and J. H. Schulman, *J. Chem. Phys.* **22**, 1063 (1954).

¹⁵J. D. Axe and P. F. Weller, *J. Chem. Phys.* **40**, 3066 (1964).

¹⁶L. G. Van Uitert and L. F. Johnson, *J. Chem. Phys.* **44**, 3514 (1966).

¹⁷R. J. Birgenau, *Appl. Phys. Letters* **13**, 193 (1968).

Electron Spin Resonance of Mn^{2+} in CaF_2 †

R. J. Richardson, Sook Lee,* and T. J. Menne

*McDonnell Douglas Research Laboratories, McDonnell Douglas Corporation,
St. Louis, Missouri 63166*

(Received 12 July 1971)

A critical investigation has been made of the room-temperature electron-spin-resonance (ESR) spectra of $^{55}Mn^{2+}$ present in dilute concentrations in CaF_2 , and a detailed quantitative explanation of this ESR center was obtained. As a result, several uncertainties associated with the previous interpretation of this center have been resolved. The theoretical spectra which fit the experimental data were obtained from a spin Hamiltonian characterized by the cubic crystal-field parameter $a = 0 \pm 0.1$ G, the manganese hyperfine constant $A = -100.8 \pm 0.1$ G, the fluorine superhyperfine constants $T_{II} = +15.3 \pm 0.1$ G and $T_I = +6.3 \pm 0.1$ G, and $g = 2.0010 \pm 0.0005$.

I. INTRODUCTION

The experimental electron-spin-resonance (ESR) spectra of Mn^{2+} substituted for the divalent cation

in fluorite-type crystals exhibit six allowed ^{55}Mn ($I = \frac{5}{2}$) hyperfine lines. In crystals containing very dilute amounts of Mn^{2+} , each of these hyperfine lines is split further into a complicated superhyper-